

# Smart $\mu$ LED Display-VLC System With a PD-Based/Camera-Based Receiver for NFC Applications

Volume 11, Number 1, February 2019

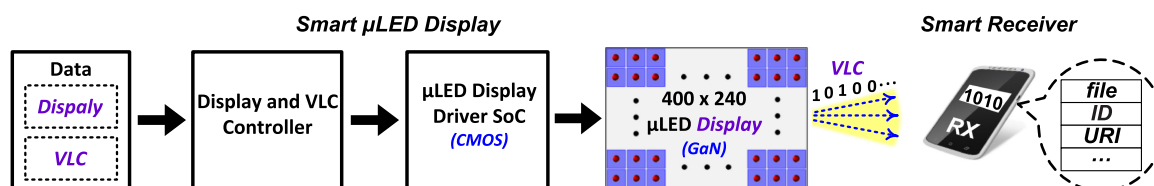
Xianbo Li, *Member, IEEE*

Babar Hussain, *Student Member, IEEE*

Jian Kang, *Student Member, IEEE*

Hoi Sing Kwok, *Fellow, IEEE*



C. Patrick Yue, *Fellow, IEEE*



DOI: 10.1109/JPHOT.2019.2892948

1943-0655 © 2019 IEEE

# Smart $\mu$ LED Display-VLC System With a PD-Based/Camera-Based Receiver for NFC Applications

Xianbo Li <sup>1,2</sup> *Member, IEEE*,  
Babar Hussain,<sup>1,2</sup> *Student Member, IEEE*,  
Jian Kang <sup>1,2</sup> *Student Member, IEEE*,  
Hoi Sing Kwok,<sup>2</sup> *Fellow, IEEE*, and C. Patrick Yue,<sup>1,2</sup> *Fellow, IEEE*

<sup>1</sup>HKUST Shenzhen Research Institute, Shenzhen 518057, China

<sup>2</sup>Department of Electronic & Computer Engineering, Hong Kong University of Science and Technology, Hong Kong

DOI:10.1109/JPHOT.2019.2892948

1943-0655 © 2019 IEEE. Translations and content mining are permitted for academic research only. Personal use is also permitted, but republication/redistribution requires IEEE permission. See [http://www.ieee.org/publications\\_standards/publications/rights/index.html](http://www.ieee.org/publications_standards/publications/rights/index.html) for more information.

Manuscript received November 29, 2018; revised January 7, 2019; accepted January 9, 2019. Date of publication January 15, 2019; date of current version February 7, 2019. This work was supported in part by the HKUST-Qualcomm Joint Innovation and Research Laboratory, in part by the State Key Laboratory on Advanced Displays and Optoelectronics Technologies in HKUST, and in part by the Science and Technology Plan of Shenzhen under Grant JCYJ20170818113929095. Corresponding author: Xianbo Li (e-mail: xlibc@connect.ust.hk).

**Abstract:** This paper presents a smart micro-light-emitting-diode ( $\mu$ LED) display system employing visible light communication (VLC) as the near-field communication technology for portable devices equipped with  $\mu$ LED displays. In the transmitter, a VLC modulator is integrated into a  $400 \times 240$  gallium nitride (GaN)  $\mu$ LED display with a pixel size of  $30 \times 30 \mu\text{m}^2$  to enable simultaneous display and VLC functions. In the receiver, two different configurations are implemented, including a photodiode (PD)-based and a smartphone camera-based receiver. The smart  $\mu$ LED display-VLC system with the two different receivers is characterized by varying the distance and the angle between the transmitter and the receiver. Experimental results show that the PD-based system can achieve a bit rate of 2 Mb/s and a maximum overall data rate of 550 kb/s beyond 10 cm, but it is sensitive to angular misalignment. In contrast, the camera-based system is more suitable for the transmission of short pieces of information at a bit rate of 16.6 kb/s, and the maximum overall data rate is 5 kb/s at a distance of 5 cm (and 2.5 kb/s when the distance is extended to 10 cm). Moreover, the camera-based system is less sensitive to angular misalignment.

**Index Terms:** Visible light communication (VLC), micro-light-emitting-diode ( $\mu$ LED) display, smart display, VLC modulator, VLC receiver, photodiode (PD), CMOS image sensor (CIS), near-field communication (NFC).

## 1. Introduction

Optical wireless communication (OWC) is expected to play an important role in the fifth-generation (5G) wireless systems to achieve higher data rates, larger network capacity, lower latency and better energy efficiency. Visible light communication (VLC) is an OWC technology that leverages the emitted light from various optoelectronic devices as the communication medium, featuring license-free operation, high-bandwidth capacity, high security and negligible electromagnetic interference [1]–[4]. With the prevalence of advanced displays as an integral part of consumer electronics, it is

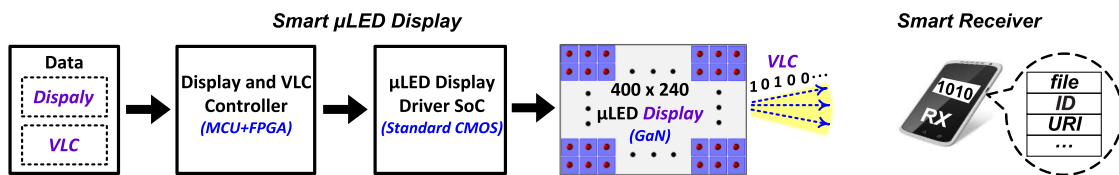


Fig. 1. Block diagram of the smart  $\mu$ LED display-VLC system.

attractive to enable displays for simultaneous VLC information delivery, meaning that display and VLC are performed at the same time, and the VLC signal can be sensed by dedicated devices without causing perceivable effects by the human eyes [5]–[7]. Recently, inorganic micro-light-emitting-diode ( $\mu$ LED) displays have demonstrated promising potential for many applications such as smartphones, smartwatches, transparent displays, augmented reality (AR) and virtual reality (VR) due to their superior performance in resolution, brightness, energy efficiency and reliability [7]–[10]. Therefore,  $\mu$ LED displays can also be turned into smart displays for inter-device communication when employing VLC [7], [11].

To detect the emitted optical signal from a smart display, different receivers can be employed, including a photodiode (PD)-based receiver and a smartphone camera-based receiver equipped with a CMOS image sensor (CIS) [11]–[14]. Usually, a low-cost PD is already sufficient to achieve a communication data rate up to tens of Mb/s [12], [13], but it requires a custom-designed receiver. In contrast, due to the low frame rate of smartphone cameras (typically 30 fps), the achievable communication data rate is limited to tens of kb/s even when taking advantage of the rolling shutter effect [5], [6], [15]. However, a camera-based receiver is able to detect the VLC signal with a larger field of view compared to the limited detection angle of a PD-based receiver, which is significant in practical applications. Another difference is that the overall data rate of the display-VLC system employing a camera-based receiver is reduced with an increased communication distance (when the projected area of the display does not occupy the entire CIS), which is not the case in the PD-based system. Nevertheless, the popularity of smartphones makes camera-based receivers more attractive for extensive usages.

This paper introduces a smart  $\mu$ LED display-VLC system for near-field communication (NFC) between portable devices equipped with  $\mu$ LED displays. In the transmitter, a VLC modulator is integrated into a  $400 \times 240$  gallium nitride (GaN)  $\mu$ LED display of which the pixel size is  $30 \times 30 \mu\text{m}^2$  [7]. In the receiver, a PD-based and a smartphone camera-based receiver are implemented [11], [16]. The whole system is demonstrated and characterized by varying the distance and the angle between the transmitter and the receiver. This is the first demonstration of a smart  $\mu$ LED display-VLC system with both a PD-based and a smartphone camera-based receiver for potential NFC applications [16]. The rest of the paper is organized as follows: the design and implementation of the system is presented in Section 2, including the system overview, the  $\mu$ LED display as the transmitter, and the PD-based/camera-based receiver. The implemented system is demonstrated in Section 3, along with various experimental results. Finally, a conclusion is drawn in Section 4.

## 2. Design and Implementation

This section covers the design and implementation details of the smart  $\mu$ LED display-VLC system, including the overview of the system, the  $\mu$ LED display as the transmitter, and two different receiver configurations.

### 2.1. Smart $\mu$ LED Display-VLC System

The block diagram of the smart  $\mu$ LED display-VLC system is illustrated in Fig. 1 [16]. On the transmitter side, both the display and the VLC data are processed and synchronized in the controller according to a custom control scheme to support simultaneous display and VLC. The controller is implemented with a micro-controller unit (MCU) and a field-programmable gate array (FPGA). The

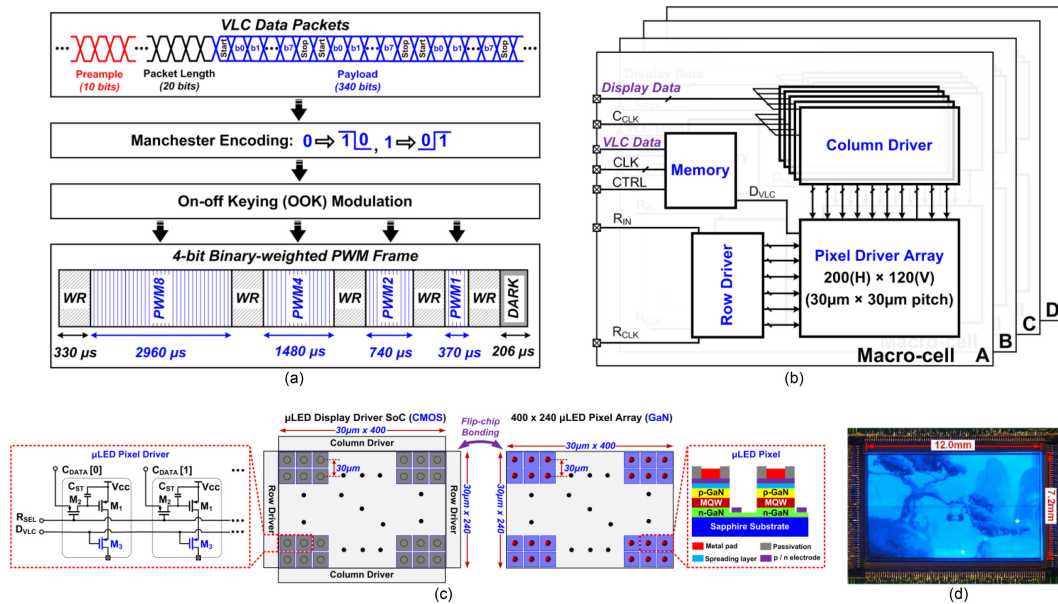


Fig. 2. (a) Frame structure that supports simultaneous display and VLC. (b) Block diagram of the smart  $\mu$ LED display driver SoC. (c) Schematic of the smart  $\mu$ LED display. (d) Photograph of the smart  $\mu$ LED display after flip-chip bonding.

data stream from the controller is then output to a  $\mu$ LED display driver system-on-a-chip (SoC) that is designed with a standard CMOS process to drive the 400 × 240 GaN  $\mu$ LED array. Finally, the display-related content is shown on the  $\mu$ LED array, and the VLC information is transmitted through the emitted light from the  $\mu$ LED display. In reality, the transmitter can be any portable device equipped with a  $\mu$ LED display, such as a smartphone or a smartwatch. On the receiver side, a PD receiver or a smartphone with a CIS camera is employed to detect the transmitted VLC information from the display, which can be a file, an identification (ID) number, a unique resource identifier (URI) and so on.

The frame structure that supports simultaneous display and VLC is depicted in Fig. 2(a) [11]. Each VLC data packet is first configured to contain a preamble sequence, the packet length information and the payload data with 370 bits in total. Then the data packets are processed with Manchester encoding (meaning each data bit is represented by the transition of two consecutive bits after encoding) to maintain a constant DC current for display. After that, on-off keying (OOK) modulation is applied to embed the VLC data packets into the four binary-weighted display sub-frames PWM8/4/2/1 that are only utilized for grayscale control in ordinary displays [7]. An SoC consisting of four macro-cells is implemented in a standard 0.5- $\mu$ m CMOS process to support the above control scheme, as shown in Fig. 2(b). Each macro-cell contains a row driver, a column driver, a 200 × 120 pixel driver array and a memory unit. As depicted in Fig. 2(c), a pixel driver unit that consists of three transistors and one capacitor (3T1C) is employed in the design, where VLC modulation is performed by the transistor M<sub>3</sub> [7]. Finally, the fabricated CMOS driver SoC is flip-chip bonded to a 400 × 240 GaN  $\mu$ LED array with a pixel size of 30 × 30  $\mu$ m<sup>2</sup> through the metal pads at the top of the pixel driver array. The smart  $\mu$ LED display after flip-chip bonding is shown in Fig. 2(d), where the GaN  $\mu$ LED array is at the top and the CMOS driver SoC is at the bottom. The size of the display core area is 12 × 7.2 mm<sup>2</sup>, and the display frame rate is designed to be 135 Hz.

## 2.2. Smart $\mu$ LED Display-VLC System With a PD-Based Receiver

As illustrated in Fig. 3(a), a PD-based receiver is designed for the smart  $\mu$ LED display-VLC system. It consists of a receiver front-end SoC to convert the detected photocurrent from the PD into a voltage

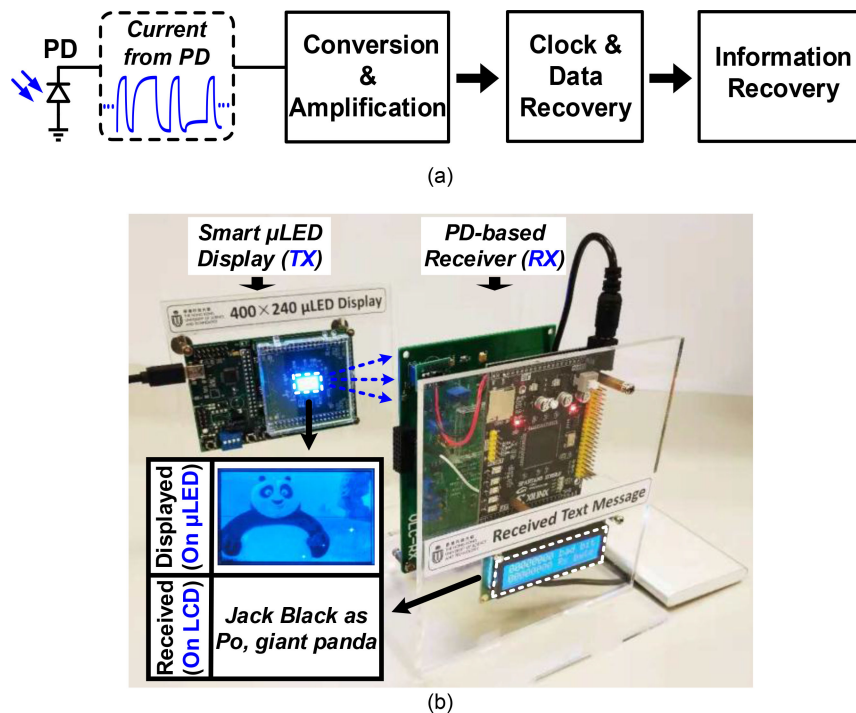


Fig. 3. (a) Block diagram of the PD-based receiver. (b) Photograph of the smart  $\mu$ LED display-VLC system with the PD-based receiver.

signal for further amplification [12], and a baseband processing unit implemented on an FPGA to execute the clock and data recovery [16]. Finally, the transmitted information is extracted based on the pre-defined data format. Fig. 3(b) is a photograph of the smart  $\mu$ LED display-VLC system employing the PD-based receiver [11], where the  $\mu$ LED display also works as a VLC transmitter when playing a video, and the PD-based receiver detects the transmitted VLC information and shows it on an LCD module. The inset in Fig. 3(b) is a screen capture of the  $\mu$ LED display and the corresponding VLC information shown on the LCD. For practical applications in the future, the  $\mu$ LED display could be part of portable consumer electronics, and the PD receiver could be integrated into a smartphone [17].

### 2.3. Smart $\mu$ LED Display-VLC System With a Camera-Based Receiver

As depicted in Fig. 4(a), another receiver based on a smartphone camera is also implemented to enable the smart  $\mu$ LED display-VLC system [16]. It consists of a CIS to capture the image of the display, and other blocks such as the graphics processing unit (GPU) to process the display and VLC information contained in the image. In order to exploit the rolling shutter effect for higher speed communication, the camera exposure time is configured to be shorter than the bit width of the VLC data. With a proper camera setting, the rolling shutter pattern with different stripes will appear on the taken images, where the bright stripe represents a logic "1" and the dark stripe represents a logic "0". The processing of the images is as follows. First, the area of the images that contains the rolling shutter pattern will be identified and be cropped to the region of interest (RoI). After RoI detection, the threshold value between different stripes will be determined to convert the stripes into a binary data stream. Finally, the embedded VLC information in the images will be recovered. Fig. 4(b) is a photograph of the smart  $\mu$ LED display-VLC system employing the camera-based receiver, where a video is played on the  $\mu$ LED display and the VLC information is transmitted concurrently. The captured image and the received data are shown on the smartphone screen.

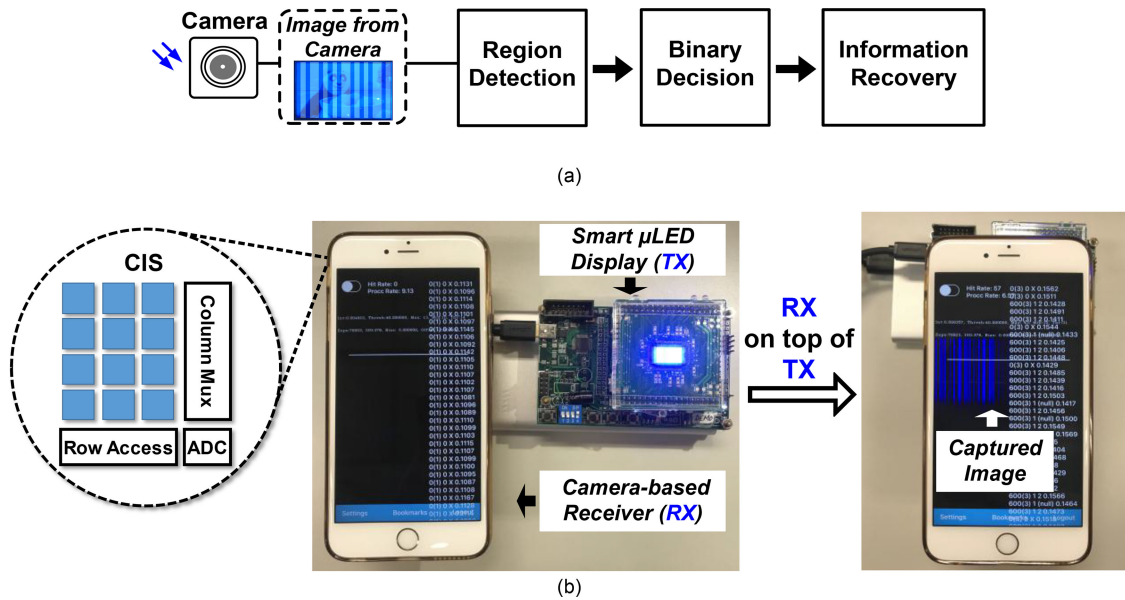


Fig. 4. (a) Block diagram of the camera-based receiver. (b) Photograph of the smart  $\mu$ LED display-VLC system with the camera-based receiver.

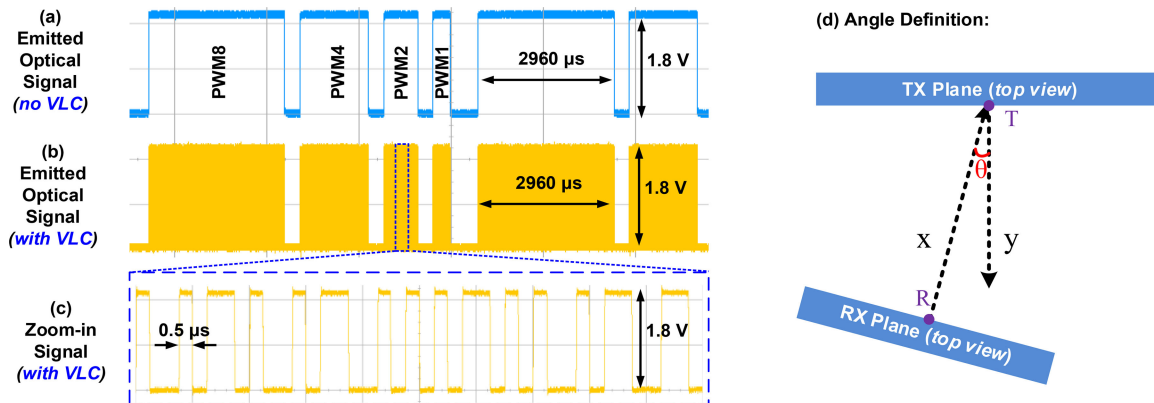


Fig. 5. Measured optical signal emitted from the smart  $\mu$ LED display: (a) The emitted optical signal without VLC modulation; (b) the emitted optical signal with VLC modulation at a bit rate of 2 Mb/s (after Manchester encoding); and (c) the zoom-in signal with VLC modulation. (d) Definition of the angle  $\theta$  between the transmitter (namely the  $\mu$ LED display) and the receiver (either the PD-based or the camera-based receiver).

### 3. Experimental Results

The measured optical signal from the smart  $\mu$ LED display using the PD-based receiver front-end SoC is presented in Fig. 5(a)–(c). In particular, Fig. 5(a) is the emitted optical signal from the display without performing VLC modulation. Therefore, only the signal for grayscale control is detected, which shows the timing of the four binary-weighted display sub-frames PWM8/4/2/1 (when the grayscale is the highest). Fig. 5(b) is the optical signal when VLC modulation is applied at a bit rate of 2 Mb/s (after Manchester encoding). The zoom-in VLC signal with a bit width of 0.5  $\mu$ s is shown in Fig. 5(c).

In order to characterize the system performance with the existence of angular misalignment, the angle between the VLC transmitter (namely the  $\mu$ LED display) and the VLC receiver (either the

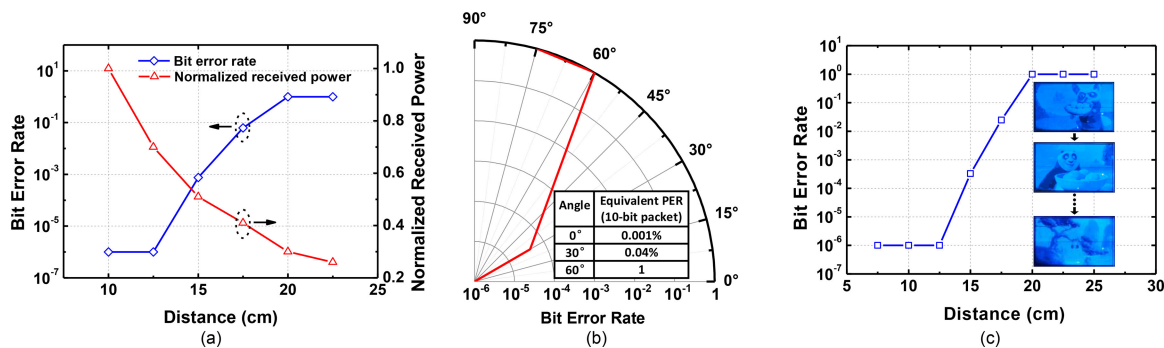


Fig. 6. For the PD-based system performing VLC at a bit rate of 2 Mb/s: (a) BER and received optical power vs. distance when the transmitter and the receiver are exactly aligned ( $\theta = 0^\circ$ ) and 25% of the pixels are turned on; (b) BER vs.  $\theta$  at a distance of 10 cm when 25% of the pixels are turned on; and (c) BER of a video clip vs. distance when the transmitter and the receiver are exactly aligned ( $\theta = 0^\circ$ ).

PD-based or the camera-based receiver) is defined, as shown in Fig. 5(d). The plane that contains the transmitter light-emission area is denoted as the TX plane, while the plane that contains the receiver light-detection area is denoted as the RX plane. In addition, T and R represent the center of the transmitter light-emission area and the center of the receiver light-detection area, respectively. By ensuring the line that passes through both T and R is always perpendicular to the RX plane, the angle  $\theta$  between the transmitter and the receiver is formed by an axis (which is y) perpendicular to the TX plane and another axis (which is x) perpendicular to the RX plane.  $\theta$  is  $0^\circ$  when the transmitter and the receiver are exactly aligned.

The performance of the smart  $\mu$ LED display-VLC system employing the PD-based receiver is presented in Fig. 6, where each VLC packet contains 370 bits with the format described in Fig. 2(a), and the bit rate is fixed at 2 Mb/s (after Manchester encoding). Fig. 6(a) is the bit error rate (BER) [16] and the normalized received optical power vs. distance when the transmitter and the receiver are exactly aligned and 25% of the  $\mu$ LED pixels are turned on (meaning that for every  $2 \times 2$  pixels, one of them is turned on). Since the received optical power is inversely proportional to the distance, the maximum distance for a BER of  $10^{-6}$  is limited to 12.5 cm. In practical applications, usually there exists angular misalignment between the smart display and the receiver. Therefore, the BER under different angles formed by the transmitter and the receiver at a distance of 10 cm is also characterized and is shown in Fig. 6(b). The result indicates a BER degradation from  $10^{-6}$  to  $4 \times 10^{-4}$  when  $\theta$  is changed from  $0^\circ$  to  $30^\circ$ . The corresponding packet error rate (PER) is increased by 40 times from 0.001% to 0.04%, assuming a packet length of 10 bits for comparison with the camera-based system. No data packet is received correctly when  $\theta$  is  $60^\circ$ , and the corresponding PER is 1. Fig. 6(c) is the BER of a 1-minute video clip vs. distance when the transmitter and the receiver are exactly aligned, achieving a BER of  $10^{-6}$  at a distance of 12.5 cm [11]. The maximum overall data rate of the PD-based system is about 550 kb/s when considering the limited time slots (PWM8/4/2/1) for VLC transmission.

The performance of the smart  $\mu$ LED display-VLC system employing the camera-based receiver is presented in Fig. 7. To match with the low detection speed of the smartphone (iPhone 6s) camera, the VLC transmission bit rate is reduced to be 16.6 kb/s, and each data packet is configured to contain 10 bits. Fig. 7(a) shows the PER [16] and the normalized received optical power vs. distance when the transmitter and the receiver are exactly aligned and 25% of the  $\mu$ LED pixels are turned on (the same display pattern is used in Fig. 6(a)). During the PER testing of the camera-based system, the same data packet is sent repeatedly, and one packet loss is counted when no packet can be successfully recovered from a single taken image. Although the incident optical power on each of the CIS pixels covered by the projected image of the  $\mu$ LED display remains constant with increased distance [14], a longer distance reduces the projected area of the  $\mu$ LED display on the CIS. Therefore, fewer data bits are recorded in each of the images, which results in the degraded

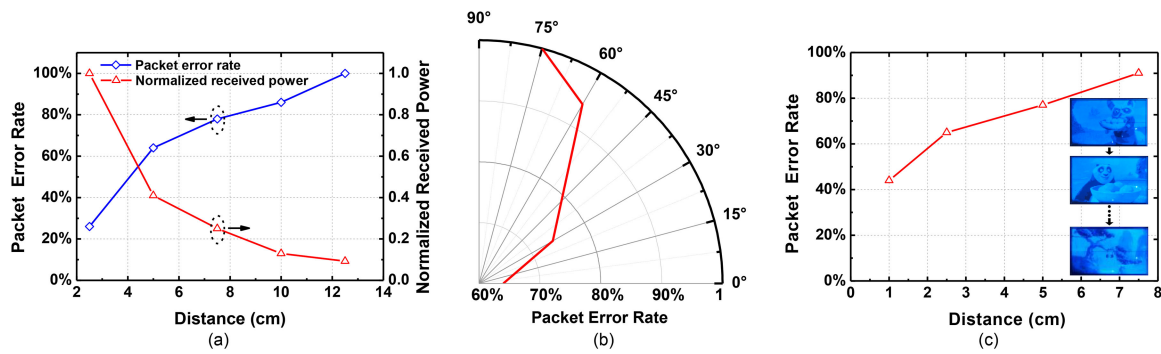


Fig. 7. For the camera-based system performing VLC at a bit rate of 16.6 kb/s: (a) PER and received optical power vs. distance when the transmitter and the receiver are exactly aligned (angle =  $0^\circ$ ) and 25% of the pixels are turned on; (b) PER vs.  $\theta$  at a distance of 5 cm when 25% of the pixels are turned on; and (c) PER of a video clip vs. distance when the transmitter and the receiver are exactly aligned (angle =  $0^\circ$ ).

PER. As shown in Fig. 7(a), the PER is increased from 64% to 86% when the distance is extended from 5 cm to 10 cm. Fig. 7(b) is the PER under different angles formed by the transmitter and the receiver at a distance of 5 cm, indicating a PER degradation from 64% to 74% when  $\theta$  is changed from  $0^\circ$  to  $30^\circ$ . The PER is further degraded to 94% when  $\theta$  is  $60^\circ$ . The result shows that the camera-based system is less sensitive to angular misalignment compared to the PD-based system. Fig. 7(c) is the PER of a 1-minute video clip (the same video is used in Fig. 6(c)) vs. distance when the transmitter and the receiver are exactly aligned, achieving a PER of about 90% at a distance of 7.5 cm. In general, a PER better than 90% can support three successful transmissions within one second when considering a typical camera frame rate of 30 fps. Therefore, it is applicable for the delivery of short pieces of information to portable devices, such as an ID number, an optical quick response (QR) code or a URI. The maximum overall data rate of the camera-based system is about 5 kb/s at a distance of 5 cm (and 2.5 kb/s at a distance of 10 cm) when considering both the available VLC transmission time and the projected area of the  $\mu$ LED display on the CIS. In practical applications, a larger  $\mu$ LED display can boost the overall data rate due to the larger projected area on the CIS, which means that more data will be recorded in each taken image. In addition, various error correction schemes can be employed to improve the PER.

#### 4. Conclusions

A smart  $\mu$ LED display-VLC system for NFC between portable devices is demonstrated and characterized in this paper. The transmitter is a  $400 \times 240$  GaN  $\mu$ LED display SoC integrated with a VLC modulator to enable simultaneous display and VLC functions. Two different receivers are implemented, including a PD-based and a smartphone camera-based receiver. Experimental results show that the PD-based system can achieve a higher data rate, but it is more sensitive to angular misalignment compared to the camera-based system. Another difference between the two systems is that, the data rate of the camera-based system is reduced with increased communication distance (when the projected area of the display does not occupy the entire CIS), which is not the case in the PD-based system (although its BER will be affected). In the future, the smart  $\mu$ LED display-VLC technique can be applied to establish an optical NFC link for data transfer between portable devices equipped with  $\mu$ LED displays, such as two smartphones, or a smartphone and a smartwatch. A higher transmission speed can be achieved by optimizing the display driver and the  $\mu$ LED array. In addition, since larger  $\mu$ LED displays are required for practical applications, the data rate and distance will be further improved. Moreover, for the PD-based system, a larger display can also be partitioned into sub-sections to support multiple-input multiple-out communication with higher throughput; for the camera-based system, the data rate can be further improved if



cameras with dedicated communication pixels are employed [17]. Therefore, it is important to integrate high-speed optical detectors into portable consumer electronics to enable future display-based OWC.

---

## References

- [1] A. V. N. Jalajakumari *et al.*, "High-speed integrated digital to light converter for short range visible light communication," *IEEE Photon. Technol. Lett.*, vol. 29, no. 1, pp. 118–121, Jan. 2017.
- [2] X. Huang, J. Shi, J. Li, Y. Wang, and N. Chi, "A Gb/s VLC transmission using hardware preequalization circuit," *IEEE Photon. Technol. Lett.*, vol. 27, no. 18, pp. 1915–1918, Sep. 2015.
- [3] B. Janjua *et al.*, "Going beyond 4 Gbps data rate by employing RGB laser diodes for visible light communication," *Opt. Exp.*, vol. 23, no. 14, pp. 18746–18753, Jul. 2015.
- [4] W. Y. Lin *et al.*, "10 m/500 Mbps WDM visible light communication systems," *Opt. Exp.*, vol. 20, no. 9, pp. 9919–9924, 2012.
- [5] B. W. Kim, H. C. Kim, and S. Y. Jung, "Display field communication: Fundamental design and performance analysis," *J. Lightw. Technol.*, vol. 33, no. 24, pp. 5269–5277, Dec. 2015.
- [6] A. Wang, C. Peng, O. Zhang, G. Shen, and B. Zeng, "InFrame: Multiflexing full-frame visible communication channel for humans and devices," in *Proc. 13th ACM Workshop Hot Topics Netw.*, Oct. 2014, p. 23.
- [7] X. Li *et al.*, "Design and characterization of active matrix LED microdisplays with embedded visible light communication transmitter," *J. Lightw. Technol.*, vol. 34, no. 14, pp. 3349–3457, Jul. 2016.
- [8] R. Horng, H. Chien, F. Tarntair and D. Wu, "Fabrication and study on red light micro-LED displays," *IEEE J. Electron Devices Soc.*, vol. 6, pp. 1064–1069, Aug. 2018.
- [9] Z. Liu *et al.*, "360 PPI flip-chip mounted active matrix addressable light emitting diode on silicon (LEDoS) micro-displays," *J. Display Technol.*, vol. 9, no. 8, pp. 678–682, Aug. 2013.
- [10] C. W. Jeon, H. W. Choi, and M. D. Dawson, "Fabrication of matrix-addressable InGaN-based microdisplays of high array density," *IEEE Photon. Technol. Lett.*, vol. 15, no. 11, pp. 1516–1518, Nov. 2003.
- [11] X. Li *et al.*, "Micro-LED display with simultaneous visible light communication function," in *Proc. SID Symp. Dig. Tech. Papers*, vol. 49, no. 1, pp. 876–879, May 2018.
- [12] X. Li *et al.*, "Design of a 2.2-mW 24-Mb/s CMOS VLC receiver SoC with ambient light rejection and post-equalization for Li-Fi applications," *J. Lightw. Technol.*, vol. 36, no. 12, pp. 2366–2375, Jun. 2018.
- [13] L. Wei, H. Zhang, and J. Song, "Experimental demonstration of a cubic-receiver-based MIMO visible light communication system," *IEEE Photon. J.*, vol. 9, no. 1, Feb. 2017, Art. no. 7900107.
- [14] T. Yamazato *et al.*, "Vehicle motion and pixel illumination modeling for image sensor based visible light communication," *IEEE J. Sel. Areas Commun.*, vol. 33, no. 9, pp. 1793–1805, Sep. 2015.
- [15] C. Liang, L. Chang, and H. H. Chen, "Analysis and compensation of rolling shutter effect," *IEEE Trans. Image Process.*, vol. 17, no. 8, pp. 1323–1330, Aug. 2008.
- [16] X. Li *et al.*, "Smart micro-LED display with synchronized information broadcast for enhanced user interaction," in *Proc. Int. Display Workshops*, Dec. 2018, pp. 421–424.
- [17] I. Takai, S. Ito, K. Yasutomi, K. Kagawa, M. Andoh, and S. Kawahito, "LED and CMOS image sensor based optical wireless communication system for automotive applications," *IEEE Photon. J.*, vol. 5, no. 5, Oct. 2013, Art. no. 6801418.